Synthesis, structure, spectral and electron-transfer properties of octahedral-$[Co^{III}(L)_2]^+/[Zn^{II}(L)_2]$ and square planar-$[Cu^{II}(L)\{OC(=O)CH_3\}]$ complexes incorporating anionic form of tridentate bis(8-quinolinyl)amine $[N^1C_9H_6–N^2–C_9H_6N^3, L^-]$ ligand

Debabrata Maiti [a], Himadri Paul [a], Nripen Chanda [a], Soma Chakraborty [a], Biplab Mondal [a], Vedavati G. Puranik [b], Goutam Kumar Lahiri [a,*]

[a] *Department of Chemistry, Indian Institute of Technology, Powai, Mumbai 400 076, India*
[b] *Physical Chemistry Division, National Chemistry Laboratory, Pune, Maharashtra 411 008, India*

Abstract

The reaction of bis(8-quinolinyl)amine $[N^1C_9H_6–N^2H–C_9H_6N^3$, LH] with $Co^{II}(ClO_4)_2 \cdot 6H_2O$ in methanol under aerobic conditions results in a new class of $[Co^{III}N_6]^+$ ($\mathbf{1}^+$) chromophore incorporating an sp^2-amido nitrogen center (N^2) in the ligand frame. During the course of the reaction, the cobalt ion has been oxidized from its starting +2 oxidation state to +3 state in **1**. The reaction of LH with the Cu-acetate yields monomeric square planar complex, $[Cu^{II}(L)\{OC(=O)CH_3\}]$ (**2**). The same copper complex **2** is also obtained from $Cu(ClO_4) \cdot 6H_2O$ in presence of CH_3COONa as base. On the other hand, the reaction of $Zn(ClO_4) \cdot 6H_2O$ with LH results in octahedral complex $Zn^{II}(L)_2$ (**3**). The Cu(II) complex **2** displays a four-line EPR spectrum at room temperature. Crystal structure of the free ligand (LH) shows that the amine proton [N(2)H] is hydrogen-bonded with the terminal quinoline nitrogen centers [N(1) and N(3)]. The crystal structure of **1** confirms the meridional geometry of the complex cation. The square planar geometry of copper complex **2** is confirmed by its crystal structure where the acetate function behaves as a monodentate ligand. The free ligand, LH, is found to be highly acidic in acetonitrile–water (1:1) medium and correspondingly the amine proton (NH) readily dissociates leading to its L^- form even in absence of any external base. The pK_b value of L^- is determined to be 2.6. Both cobalt and copper complexes do not show any expected spin-allowed d–d transitions, possibly have masked by the intense charge-transfer transitions. However, in case of cobalt complex **1**, one very weak unusual spin-forbidden $^1A_{1g} \rightarrow {}^3T_{1g}$ transition has been observed at 935 nm. The quasi-reversible cobalt (III) $\leftrightharpoons$ cobalt(II) reduction of **1** is observed at E^0, −1.0 V versus SCE.

Keywords: Cobalt; Copper; Zinc; Bis(8-quinolinyl)amine; Structures

1. Introduction

Although the ligand bis(8-quinolinyl)amine, LH, was synthesized long back [1,2], the complexation property of LH has been studied only recently to a little extent. The first metal complex of L^- was reported to be a tetrahedral copper-complex, $[Cu^{II}(L)Cl]$ [2]. The crystal structure of the complex reveals the presence of a pairwise interaction between the monomeric units in the solid state, where each ionized amine group occupies an apical co-ordination site of the second Cu(II) center producing a square pyramidal geometry around each copper unit. The crystal structure of the lithium complex of L^- shows a dimeric structure $[Li_2(L)_2]$ in which the two lithium ions and two bridging amido nitrogen centers join together to form a parallelepiped that bisects

the dimeric complex, whereas the corresponding Tl^{I} complex Tl(L) exists in the monomeric form [3]. The ligand L^- behaves like a pincer ligand with the divalent Ni^{2+}, Pd^{2+} and Pt^{2+} and the Pt^{2+}complex is reported to perform C–H bond activation process of benzene ring in the presence of a base [4]. The metal complexes of L^- have been essentially restricted to tetra-coordinated species so far, therefore, the present work primarily deals with the hexa-coordinated Co^{III}, Zn^{II} and tetra-coordinated Cu^{II} complexes incorporating L^-.

Herein, we report the synthesis and characterizations of octahedral $[Co^{III}(L)_2]^+$ (**1**), $[Zn^{II}(L)_2]$ (**3**) and square planar $[Cu^{II}(L)\{OC(=O)CH_3\}]$ (**2**) complexes, crystal structures of the free ligand (LH), cobalt and copper complexes and their spectral/electrochemical properties.

2. Experimental

2.1. Materials

Cobalt carbonate and copper nitrate were converted into cobalt perchlorate hexahydrate and copper perchlorate hexahydrate, respectively, by using perchloric acid. 8-Amino quinoline and 8-hydroxy quinoline were purchased from Aldrich, USA. Other chemicals and solvents were reagent grade and used as received. For electrochemical studies, HPLC grade acetonitrile was used. Commercial tetraethyl ammonium bromide was converted to pure tetraethylammonium perchlorate (TEAP) by following an available procedure [5].

2.2. Physical measurements

Solution electrical conductivity was checked using a Systronic conductivity bridge-305. Electronic spectra were recorded using Shimadzu UV-160 (1100–200 nm) and UV-2100 (900–200 nm) spectrophotometer. IR spectra were recorded on a Nicolet spectrophotometer with samples prepared as KBr pellets. ^{1}H NMR spectra were obtained with a 300-MH_z Varian spectrometer. Cyclic voltammetric and coulometric measurements were carried out using a PAR model 273A electrochemistry system. A platinum wire working electrode, a platinum wire auxiliary electrode and a saturated calomel reference electrode (SCE) were used in a standard three-electrode configuration. TEAP was the supporting electrolyte and the solution concentration was ca. 10^{-3} M; the scan rate used was 50 mV s^{-1}. A platinum gauze working electrode was used for coulometric experiments. All electrochemical experiments were carried out under dinitrogen atmosphere, and all redox potentials are uncorrected for junction potentials. The elemental analyses were carried out with a Perkin–Elmer 240C elemental analyzer.

2.3. Preparation of ligand and complexes

2.3.1. Preparation of LH $[N^1C_9H_6–N^2H–C_9H_6N^3]$

The ligand, LH, was synthesized by a modified Bucherer reaction [1,2].

2.3.2. Preparation of $[Co(N^1C_9H_6–N^2–C_9H_6N^3)_2](ClO_4)$ (**1**)

To a solution of $Co(ClO_4)_2 \cdot 6H_2O$ (100 mg, 0.273 mmol) in methanol, the ligand, LH (185 mg, 0.682 mmol), was added. The reaction mixture was stirred magnetically for a period of 4 h. The brown colored solid thus obtained was filtered off and washed thoroughly with cold methanol followed by cold water. The product was dried over P_4O_{10} under vacuo. The complex **1** was then recrystallized from benzene–acetonitrile (1:1) mixture. Yield: 124 mg (65%). *Anal.* Calc. for **1**: C, 61.86; H, 3.46; N, 12.02. Found: C, 61.46; H, 3.58; N, 11.40%. Λ_M (Ω^{-1} cm^2 mol^{-1}) in CH_3CN; 117. [^{1}H NMR data in $CDCl_3$: δ, ppm (J, H_z): H(2), 8.45(7.8); H(4), 8.08(8.4); H(5), 8.0(5.1); H(3), 7.85(7.8, 8.4); H(7), 7.26(9.6); H(6), 7.16(5.4, 5.4)].

2.3.3. $[Cu(N^1C_9H_6–N^2–C_9H_6N^3)\{OC(=O)CH_3\}]$ (**2**)

The ligand, LH (156 mg, 0.575 mmol), was added to a methanolic solution of anhydrous copper acetate (50 mg, 0.275 mmol) under stirring condition. The reaction mixture was stirred magnetically for a period of 6 h. The reddish brown colored solid thus formed was filtered off and washed thoroughly with cold methanol followed by cold water. The product was then dried over P_4O_{10} under vacuo. The complex **2** was purified by recrystallization from dichloromethane–hexane (1:1) mixture. Yield: 66 mg (61%). *Anal.* Calc. for **2**: C, 61.14; H, 3.85; N, 10.69. Found: C, 60.43; H, 4.03; N, 11.12%.

2.3.4. $[Zn(N^1C_9H_6–N^2–C_9H_6N^3)_2]$ (**3**)

To a solution of $Zn(ClO_4)_2 \cdot 6H_2O$ (100 mg, 0.268 mmol) in methanol was added LH (160 mg, 0.589 mmol). The reaction mixture was stirred magnetically for a period of 4 h. The red colored solid thus obtained was filtered off and washed thoroughly with cold methanol followed by cold water. The product was dried over P_4O_{10} under vacuo. The complex **3** was then recrystallized from dichloromethane–hexane (1:1) mixture. Yield: 94 mg (58%). *Anal.* Calc. for **3**: C, 71.35; H, 3.99; N, 13.87. Found: C, 70.66; H, 3.55; N, 14.15%. ^{1}H NMR data in $CDCl_3$: δ, ppm (J, H_z): H(2), 8.19(8.1); H(4), 8.00(5.9); H(5), 7.92(8.3); H(3), 7.59(8.1, 8.1); H(7), complex multiplet centered at δ, 6.95 ppm; H(6), complex multiplet centered at δ, 6.95 ppm.

2.4. X-ray structure determination

The single crystals of LH were grown by slow evaporation of dichloromethane solution of LH. The single

Table 1
Crystallographic data for $[NC_9H_6–NH–C_9H_6N$ (LH)], $[Co^{III}(L)_2]ClO_4 \cdot 0.5C_6H_6$ (**1**) and $[Cu^{II}(L)\{OC(=O)CH_3\}]$ (**2**)

Formula	$C_{18}H_{13}N_3$	$C_{39}H_{27}N_6ClO_4Co$	$C_{20}H_{15}N_3O_2Cu$
M	271.31	738.07	392.89
Crystal symmetry	monoclinic	triclinic	triclinic
Space group	$C2/c$	$P\bar{1}$	$P\bar{1}$
a (Å)	31.858(3)	9.0439(8)	7.9970(6)
b (Å)	6.2360(4)	12.5407(9)	9.8040(7)
c (Å)	14.5940(10)	14.8085(11)	11.2770(14)
α (°)		101.484(6)	75.217(7)
β (°)	111.524(7)	91.498(7)	85.585(8)
γ (°)		90.455(7)	73.918(6)
V (Å^3)	2697.1(4)	1645.2(2)	821.41(13)
T (K)	293(2)	293(2)	293(2)
μ (mm^{-1})	0.081	0.657	1.350
Z	8	2	2
R_1	0.0455	0.0577	0.0309
wR_2	0.0906	0.1363	0.0769

crystals of complex **1** were grown by slow diffusion of an acetonitrile solution of it in benzene followed by slow evaporation at 298 K. Single crystals of copper complex **2** were grown by slow diffusion of dichloromethane solution of **2** into hexane followed by slow evaporation at 298 K. The X-ray data were collected on a PC-controlled Enraf–Nonius CAD-4 (MACH-3) single crystal X-ray diffractometer using Mo Kα radiation. Significant crystal data and data collection parameters are shown in Table 1. The structures were solved by direct method using SHELXS 86 and refined by full-matrix least-squares on F^2 using SHELXL 97 [6]. The X-ray analysis of the complex **1** shows one ClO_4^- anion and half molecule of benzene as solvent of crystallization in the asymmetric unit. The solvent molecule of benzene is found to be highly disordered and hydrogen atoms for this solvent have not been fixed.

3. Results and discussion

3.1. Synthesis and characterization

The ligand bis(8-quinolinyl)amine $[N^1C_9H_6–N^2H–C_9H_6N^3$, LH] comprising one dissociable amine proton (N^2H) has been synthesized from 8-aminoquinoline and 8-hydroxyquinoline following the reported procedure [1,2]. The direct bonding of N^2 center with the two-electron-withdrawing quinoline moieties makes the amine proton (N^2H) in LH substantially acidic. Thus, the NH proton of LH dissociates in acetonitrile–water (1:1) mixture to give the corresponding conjugate base (L^-). In view of that, the UV–Vis spectrum of the free ligand in 1:1 acetonitrile–water fails to show any noticeable changes in spectral behavior on increasing pH. Therefore the pK_b of L^- of 2.6 has been determined by *pH*-titration (Fig. 1). The strong acidic nature of LH facilitates the dissociation of the NH function under

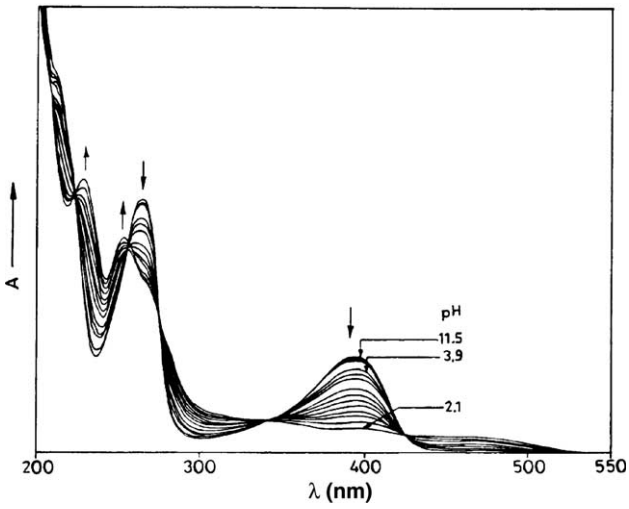

Fig. 1. Electronic spectra of LH at different pH in 1:1 acetonitrile–water. The arrows indicate increase or decrease in band intensities as the reaction proceeds.

normal reaction conditions (Scheme 1). However, in case of peptide bound amide proton [C(=O)–NH] the presence of a base ($NaOCH_3$ or NaOH) is necessary to deprotonate the –NH proton during metallation process [7]. The complex $[Co^{III}(L)_2]ClO_4$ (**1**) has been synthesized from $Co^{II}(ClO_4)_2 \cdot 6H_2O$ and LH in methanol solvent under aerobic condition (Scheme 1). The synthesis of **1** from cobalt (II) starting salt is attained with the metal oxidation. In view of the low Co(III)–Co(II) reduction potential of **1** (see later) it may be logically considered that aerial oxygen is the most probable oxidant [8]. Under a strict dinitrogen atmosphere corresponding cobalt(II) species $\mathbf{1}^-$ can be generated, however, $\mathbf{1}^-$ is found to be oxidized spontaneously in contact with slight amount of air.

The reaction of LH with copper acetate or copper perchlorate in presence of sodium acetate base results in mononuclear tetra-coordinated copper (II) complex of the composition $Cu^{II}(L)\{^-O–C(=O)CH_3\}$ (**2**) (Scheme 1). On the other hand, the reaction of zinc perchlorate hexahydrate with the ligand, LH, yields bis-octahedral neutral complex $Zn^{II}(L)_2$ (**3**) as like the cobalt complex (Scheme 1).

The cobalt and zinc complexes are diamagnetic and behave as 1:1 conductor and neutral, respectively, in acetonitrile. The electrically neutral copper complex **2** exhibits one-electron paramagnetism ($\mu = 1.87$ BM). All the complexes exhibit satisfactory elemental analysis (Section 2).

3.2. Crystal structures of the free ligand $NC_9H_6–NH–C_9H_6N$ (LH), $[Co^{III}(L)_2]ClO_4$ (1) and $[Cu^{II}(L)\{OC(=O)CH_3\}]$ (2)

The formation of LH was confirmed by its crystal structure determination. Crystal structure is shown in

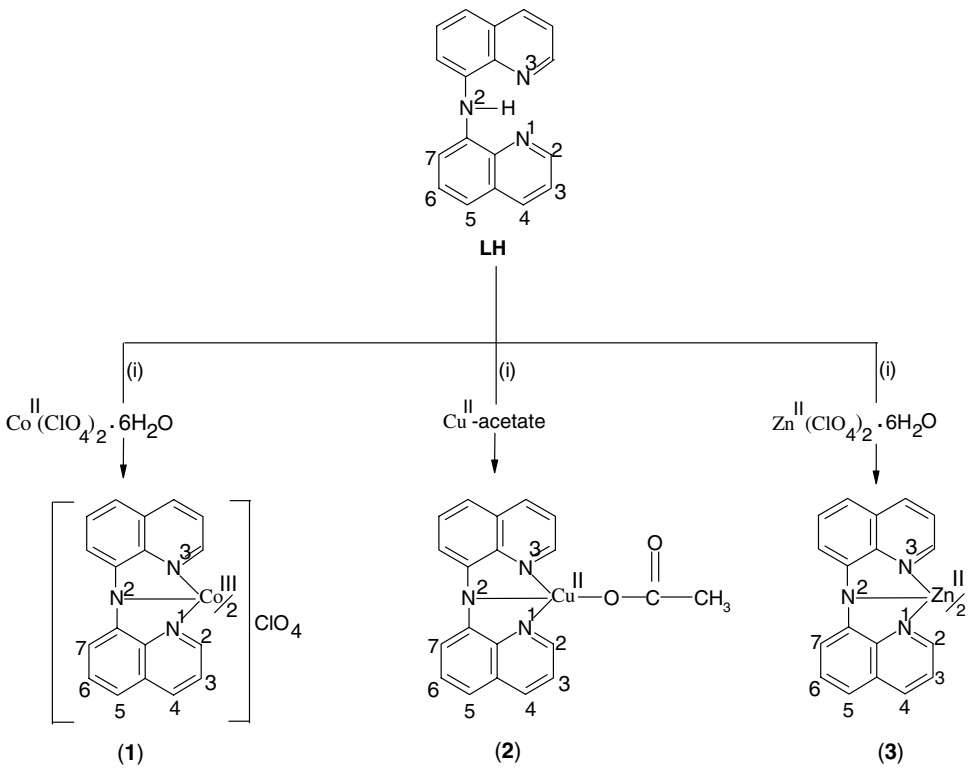

Scheme 1. (i) MeOH, stir.

Fig. 2 and selective bond distances and angles are shown in Table 2. The bond distances and angles are unremarkable. The amido proton N(1)–H(101) has formed intramolecular hydrogen bonding with the nearby two quinolinic nitrogen centers [N(2) and N(3)] (Table 3).

The crystal structure of $[Co^{III}(L)_2]ClO_4 \cdot 0.5C_6H_6$ (**1**) is shown in Fig. 3. Selected bond distances and angles are listed in Table 2. The lattice consists of one type of molecule. The crystal consists of an array of $[Co(L)_2]^+$ cations, $[ClO_4]^-$ anions and benzene of crystallization in a ratio of 1:1:0.5 stoichiometry. The coordination geometry around the cobalt ion is distorted octahedral. The tridentate anionic ligand (L^-) is bonded to the cobalt ion with the terminal quinoline nitrogen atoms being *trans* to each other. The central amido nitrogen centers [N(1) and N(5)] of two L^- around the metal ion are also in *trans* configuration. The two meridional planes are nearly orthogonal. The sp^2 hybridization about each ionized amine group is reflected by the angles Co–N(1)–C(1), Co–N(1)–C(17), C(1)–N(1)–C(17), Co–N(5)–C(26), Co–N(5)–C(28), C(26)–N(5)–C(28), corresponding to 114.9(3)°, 114.1(4)°, 131.0(5)°, 114.6(4)°, 115.7(4)° and 129.6(5)°, respectively. The *trans* angles N(2)–Co–N(3), N(4)–Co–N(6) and N(1)–Co–N(5) are 168.7(2)°, 168.9(2)° and 178.71(19)°, respectively. The observed Co^{III}–N(quinoline) bond distances [1.913(4)–1.929(4) Å] are shorter than the average Co^{III}–N(pyridine) bond distances [1.94–2.00 Å] [9]. The Co-ionized amine bond distances [Co–N(1), 1.889(4) Å and Co–N(5), 1.879(5) Å] are reasonably shorter than the Co–quinoline N bond distances [Co–N(2), 1.913(4) Å; Co–N(3), 1.929(4) Å; Co–N(4), 1.921(4) Å and Co–N(6), 1.916 Å]. The Co^{III}–N(ionized amine) distances in **1** are appreciably shorter than the observed Co^{III}–NH distances [1.929(7)–1.951(7) Å] [10] and Co^{III}–N(amido) distances [1.929(6)–1.942(3)] [11] which are due to the fact of enhanced π-donor property of the ionized amino function. The perchlorate anion is tetrahedral with an average Cl–O distance of 1.410(6) Å and an average O–Cl–O angle of 109.46(4)°.

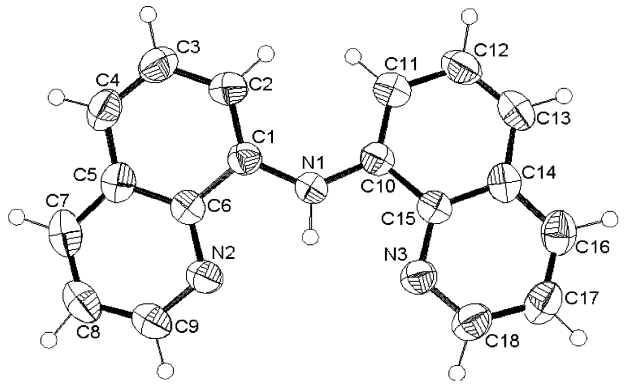

Fig. 2. Crystal structure of $[NC_9H_6–NH–C_9H_6N$, (LH)].

The packing diagram of the complex molecule **1** shows several intramolecular C–H···N and intermolecular C–H···O hydrogen bonding patterns (Table 3). The

Table 2
Selected bond distances and angles and their standard deviation for $[NC_9H_6–NH–C_9H_6N$, (LH)], $[Co(L)_2]ClO_4 \cdot 0.5C_6H_6$ (**1**) and $[Cu(L)\{OC(=O)CH_3\}]$ (**2**)

$NC_9H_6–NH–C_9H_6N$ (LH)		$[Co^{III}(L)_2]ClO_4 \cdot 0.5C_6H_6$		$[Cu^{II}(L)\{OC(=O)CH_3\}]$ (**2**)	
Bond distances (Å)					
N(1)–C(10)	1.382(3)	Co–N(1)	1.889(4)	Cu(1)–N(2)	1.932(2)
N(1)–C(1)	1.385(3)	Co–N(2)	1.913(4)	Cu(1)–O(1)	1.9495(18)
N(2)–C(9)	1.331(3)	Co–N(3)	1.929(4)	Cu(1)–N(3)	1.982(2)
N(2)–C(6)	1.365(3)	Co–N(4)	1.921(4)	Cu(1)–N(1)	1.983(2)
N(3)–C(18)	1.322(3)	Co–N(5)	1.879(5)	O(1)–C(19)	1.272(3)
N(3)–C(15)	1.369(3)	Co–N(6)	1.916(4)	O(2)–C(19)	1.226(3)
Bond angles (°)					
C(10)–N(1)–C(1)	132.4(2)	N(5)–Co–N(1)	178.71(19)	N(2)–Cu(1)–O(1)	175.34(9)
N(1)–C(1)–C(6)	115.4(2)	N(5)–Co–N(2)	96.01(19)	N(2)–Cu(1)–N(3)	82.77(9)
N(2)–C(6)–C(1)	117.3(2)	N(1)–Co–N(2)	84.37(19)	N(2)–Cu(1)–N(1)	82.72(9)
C(9)–N(2)–C(6)	117.1(2)	N(5)–Co–N(6)	84.1(2)	N(3)–Cu(1)–N(1)	164.50(9)
C(2)–C(1)–N(1)	126.7(2)	N(1)–Co–N(6)	94.7(2)	O(1)–Cu(1)–N(3)	98.03(9)
C(2)–C(1)–C(6)	117.9(2)	N(2)–Co–N(6)	89.82(18)	O(1)–Cu(1)–N(1)	96.87(9)
N(1)–C(10)–C(15)	115.5(2)	N(5)–Co–N(4)	84.97(19)	C(19)–O(1)–Cu(1)	107.81(17)
C(10)–C(15)–N(3)	117.3(2)	N(1)–Co–N(4)	96.27(19)	O(2)–C(19)–O(1)	123.7(3)
C(18)–N(3)–C(15)	117.2(2)	N(2)–Co–N(4)	89.63(17)	C(8)–N(2)–C(17)	128.9(2)
C(11)–C(10)–N(1)	126.7(2)	N(1)–Co–N(3)	84.5(2)	O(1)–C(19)–C(20)	116.6(3)
C(11)–C(10)–C(15)	117.8(2)	N(2)–Co–N(3)	168.7(2)		
		N(6)–Co–N(3)	92.45(18)		
		N(4)–Co–N(3)	90.24(17)		
		N(6)–Co–N(4)	168.9(2)		
		N(5)–Co–N(3)	95.2(2)		
		C(1)–N(1)–C(17)	131.0(5)		
		C(28)–N(5)–C(26)	129.6(5)		

Table 3
Hydrogen bonds for $NC_9H_6–NH–C_9H_6N$ (LH) and $[Co^{III}(L)_2]ClO_4 \cdot 0.5C_6H_6$ [Å and (°)]

	D–H···A (°)	*d*(D–H) Å	*d*(H···A) Å	*d*(D···A) Å	D–H···A (°)
$NC_9H_6–NH–C_9H_6N$ (LH)					
Intra- molecular	N(1)–H(101)···N(2)	0.9383	2.1691	2.6592	111.41
	N(1)–H(101)···N(3)	0.9383	2.1984	2.6626	109.48
*$[Co^{III}(L)_2]ClO_4 \cdot 0.5C_6H_6$ (**1**)*					
Intra-molecular	C(8)–H(8)···N(5)	0.97	2.618	3.054	107.45
	C(10)–H(10)···N(5)	0.85	2.606	3.026	111.56
	C(19)–H(19)···N(1)	0.97	2.533	3.080	115.56
	C(35)–H(35)···N(1)	0.98	2.515	3.002	110.37
Inter-molecular	C(16)–H(16)···O(4)^{i}	0.99	2.430	3.305	146.74
	C(30)–H(30)···O(3)^{ii}	0.99	2.533	3.406	146.10

^{i}, $1-x$, $-y$, $1-z$ and ^{ii}, x, y, $-1+z$.

O(3) and O(4) atoms of the perchlorate moiety are involved in intermolecular C–H···O hydrogen bonds, sandwiching the solvent benzene molecule sitting on the symmetry position.

The formation of copper complex **2** has been confirmed by its single crystal X-ray structure. The crystal structure is shown in Fig. 4 and selected bond distances and angles are given in Table 2. The lattice consists of one type of molecule. The square planar geometry around the copper ion in $Cu^{II}N_3O$ coordination environment is evidenced from the angles subtended around the copper center (Table 2). The planarity of coordinated L^- is essentially leading to the square planar geometry. The tridentate anionic ligand is bonded to the copper ion with the terminal quinoline nitrogen centers [N(1) and N(3)] and the central amido nitrogen [N(2)]. The sp^2 hybridization of the ionized amine group is confirmed by the angles Cu(1)–N(2)–C(17), 115.5(17)°; Cu(1)–N(2)–C(8), 115.5(17)° and C(8)–N(2)–C(17), 128.9(2)°. The substantial deviation of the C(8)–N(2)–C(17) angle [128.9(2)°] of the coordinated tridentate ligand (L^-) with respect to the expected sp^2 angle of 120° possibly can account for the observed significant decrease in N–Cu–N *cis* angles [N(1)–Cu(1)–N(2), 82.72(9)° and N(2)–Cu(1)–N(3), 82.77(9)°]. The *trans* angles N(2)–Cu(1)–O(1) and N(1)–Cu(1)–N(3) are

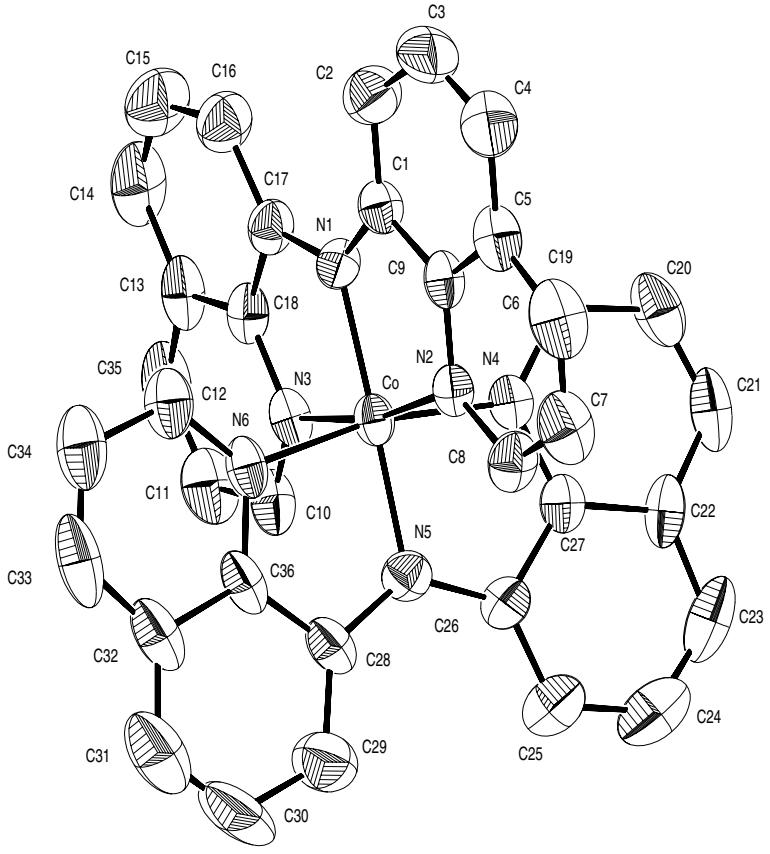

Fig. 3. Crystal structure of $[Co^{III}(L)_2]ClO_4 \cdot 0.5C_6H_6$ (**1**).

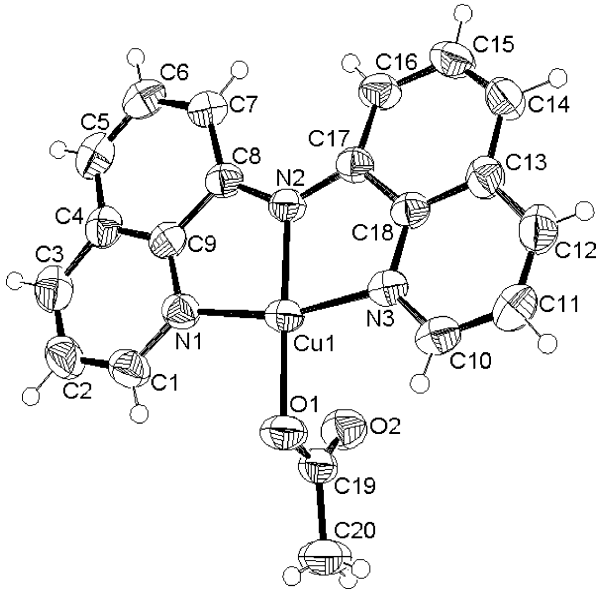

Fig. 4. Crystal structure of $[Cu^{II}(L)\{OC(=O)CH_3\}]$ (**2**).

175.3(9)° and 164.5(9)°, respectively. The Cu^{II}–N (quinoline) distances [Cu(1)–N(1), 1.983(2) Å and Cu(1)–N(3), 1.982(2) Å] are reasonably longer than the corresponding Cu(1)–N(2) (ionized amido nitrogen), 1.932(2) Å which reflects the π-donor ability of the ionized amino function. The Cu(II)–N (quinoline) distances are comparable with those of reported Cu(II)–N (quinoline) distances, 1.972–2.033Å [12]. Cu(1)–O(1) (acetate) distance 1.9495(18) Å is matched well with the reported data of other Cu(II)-monodentate acetate complexes [13]. It is to be noted that the crystal structure of similar reported tetracoordinated $Cu^{II}(L)Cl$ complex shows dimeric interaction through the ionized sp^2 hybridized amido nitrogen [2]. It was proposed that the filled p_z orbital of the sp^2 hybridized amido nitrogen is sufficiently basic to bind to a second copper ion resulting in dimerization. However, any sort of dimerization process has not been observed in the present case which implies that in comparison to the chloro complex the basicity of the amido nitrogen in **2** is significantly less, although the Cu–N(amido nitrogen) distance is almost same in both the complexes [1.932 (2)Å in **2** and 1.935 (2)Å in the corresponding chloro complex $[Cu^{II}(L)Cl]$] [2].

3.3. Spectral properties

The perchlorate vibrations of **1** appeared at 1093 and 629 cm^{-1} in the IR spectrum.

The ^{1}H NMR spectra of **1** and **3** in $CDCl_3$ solvent reveal that half of the individual ligand (L^-) represents the whole molecule due to the presence of internal symmetry (Fig. 5). The absence of NH proton of LH in the NMR spectra supports the bonding of anionic form of the ligand (L^-) to the metal ion in the solution state as well.

The acetonitrile solution of **1** exhibits multiple intense transitions in the UV–Vis region (Fig. 6(a)). [λ_{max}/nm (ε/$M^{-1}\,cm^{-1}$): 505(25 000), 431(9700), 374(5050), 292(57 000) and 217(107 000)]. Based on the high intensities of the visible bands the transitions are assigned to be charge-transfer in nature [14]. Since Co(III) is in the low-spin t_{2g}^6 configuration, the visible energy intense bands at 505 and 431 nm are, therefore, assigned as $L^- \rightarrow e_g(Co^{III})$ ligand-to-metal charge-transfer transitions [8,15]. The UV region moderately strong band at 372 nm and strong bands at 292 and 217 nm are presumably due to intra ligand $n \rightarrow \pi^*$ and $\pi \rightarrow \pi^*$ transitions, respectively [16]. The free ligand (LH) also exhibits strong transitions in the UV-region [λ_{max}/nm (ε/

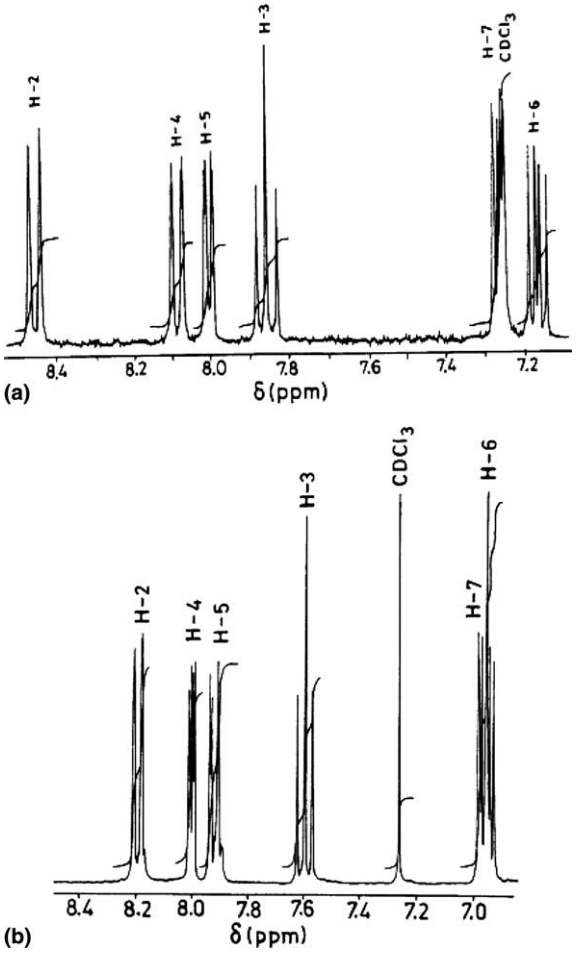

Fig. 5. ^{1}H NMR spectra of: (a) $[Co^{III}(L)_2]ClO_4$ (**1**) and (b) $Zn^{II}(L)_2$ (**3**) in $CDCl_3$.

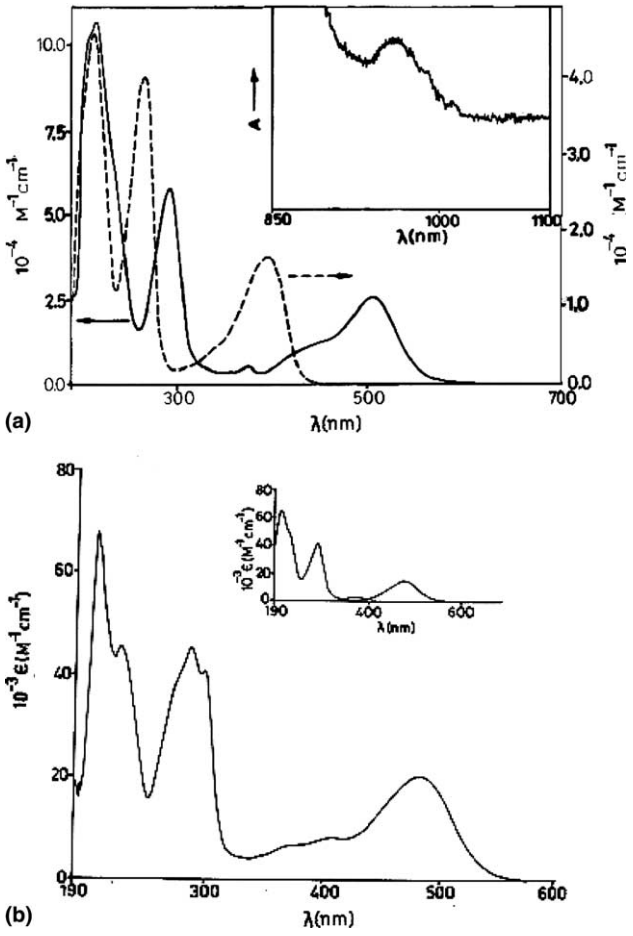

Fig. 6. Electronic spectra of: (a) $[Co^{III}(L)_2]ClO_4$ (**1**) (——) and LH (- - - - -), inset shows the electronic spectrum of **1** in the range of 1100–850 nm; (b) $Zn^{II}(L)_2$ (**3**), inset shows the spectrum of $[Cu^{II}(L)\{OC(=O)CH_3]$ (**2**) in acetonitrile.

$M^{-1}\,cm^{-1}$): 397(16 100); 264(38 900); 214(44 700) in CH_3CN (Fig. 6(a))].

For low-spin octahedral Co(III) complexes having CoN_6 coordination environment the expected two d–d transitions, $^1A_{1g} \rightarrow {}^1T_{1g}$ and $^1A_{1g} \rightarrow {}^1T_{2g}$ usually appear near 500 nm and at a higher energy part, respectively ($\varepsilon \sim 10$–300 $M^{-1}\,cm^{-1}$) [17]. Accordingly, the $[Co(trpy)_2]^{3+}$ and Co(III)-peptide complexes exhibit lowest energy $^1A_{1g} \rightarrow {}^1T_{1g}$ transition near 500 nm [7a,18]. However, in **1** no such d–d transitions are detected in the UV–Vis region. The appearance of low energy intense charge-transfer transitions possibly have masked the expected weak d–d bands [8,19]. On the other hand **1** exhibits a very weak band at 955 nm (ε/$M^{-1}\,cm^{-1}$, 11]) (Fig. 6(a), inset). The existence of spin-allowed d–d band at an energy which is much lower than the observed lowest energy LMCT transition ($\lambda = 505$ nm) particularly in an environment consisting of potent electron-rich ligand function (L^-) and the metal ion in relatively higher oxidation state (Co^{3+}) is hard to conceive. It may, therefore, be logical to look for the possible correspondence of the 955-nm band with the

$^1A_{1g} \rightarrow {}^3T_{1g}$ spin-forbidden singlet–triplet transition as an alternative approach. The characteristics of very weak and relatively low energy of the 955 nm band can possibly justify its origin as $^1A_{1g} \rightarrow {}^3T_{1g}$ spin-forbidden transition. It may be noted that the spin-forbidden singlet–triplet transitions have been detected earlier in few other $Co^{III}N_6$ systems such as $Co(NH_3)_6^{3+}$ and $Co(en)_3^{3+}$ complexes [17,20].

The complex **2** exhibits four intense transition in the UV–Vis region (Fig. 6(b), inset): [λ_{max}/nm (ε/M^{-1} cm^{-1}): 476(14 622), 362(2781), 284(42 625) and 206(65 872)]. The intense transitions are believed to be charge transfer in nature. The lowest energy transition at 476 nm possibly originated from $L^- \rightarrow (Cu^{II})$ LMCT transition. The UV region transitions are possibly originated via intraligand $\pi \rightarrow \pi^*$ and $n \rightarrow \pi^*$ transitions. The expected weak d–d transition in the visible region for **2** has not been detected even with its concentrated solution. It may be lost in the low-energy tail of the intense charge-transfer transition at 476 nm.

The complex **3** shows multiple transitions in the UV–Vis region (Fig. 6(b)): λ_{max}/nm (ε/M^{-1} cm^{-1}): 482(20 227), 229(40 568), 287(45 454), 228(45 340) and 207(67 272). In view of their high intensities the transitions are believed to be charge transfer in nature.

The EPR spectrum (Fig. 7) of **2** is recorded in 1:1 chloroform–toluene mixture at 298 K and it displays an equally spaced four-line spectrum (g_{av}, 2.106 and A_{av}, 80 G) due to hyperfine splitting by the copper nucleus ($I = 3/2$) [21].

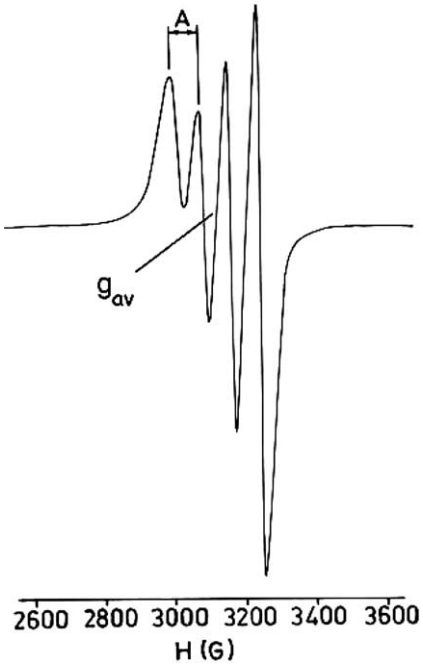

Fig. 7. EPR spectrum of $[Cu^{II}(L)\{OC(=O)CH_3\}]$ (**2**) in 1:1 chloroform–toluene mixture at 298 K.

3.4. Electron-transfer properties

Redox properties of $[Co^{III}(L)_2]^+$ (**1**) and $[Cu^{II}(L)\{OC(=O)CH_3\}]$ (**2**) have been examined in acetonitrile solvent using platinum wire working electrode (Figs. 8 and 9). Cobalt complex **1** displays one quasi-reversible one-electron reductive process E^0, $V(\Delta E_p, mV)$ at −1.0(100) versus SCE (couple-III) (Fig. 8(a)) which is assigned to be $Co(III) \leftrightharpoons Co(II)$ couple. The high negative potential (<−1.0 V) of cobalt(III)–cobalt(II) reduction process can account for the preferential stabilization of cobalt ion in +3 oxidation state in **1** under atmospheric conditions. The cobalt(III)–Cobalt(II) reduction potential of the similar bis octahedral peptido complex {$[Co(L)_2]^+$, $L^- = N$-(2-(4-imidazolyl)ethyl)-pyridine-2-carboxamide} appears at −0.62 V in MeOH, −0.72 V in $(CH_3)_2SO$ and −0.69 V in DMF (acetonitrile data is not available) [22]. The substantial negative shift of Co(III)–Co(II) reduction potential (∼0.3 V) while moving from the deprotonated amido complex to the deprotonated amino complex **1** implies the reasonable difference in basicity between the two sp^2 nitrogen centers. Thus, in case of peptide bound amide proton [C(=O)–NH] the oxidation of cobalt(II) to cobalt(III) takes place only via bubbling of air through the reaction mixture and in the presence of a base ($NaOCH_3$ or NaOH) [22]. The electrochemically generated Co(II) congener $[Co(L)_2]$ ($\mathbf{1}^-$) has been found to be quite unstable, it spontaneously oxidizes to the parent $[Co^{III}(L)_2]^+$ state which has essentially

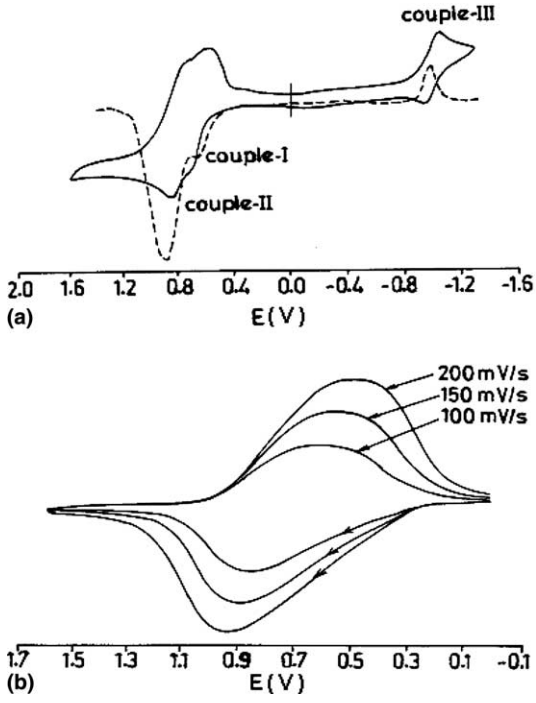

Fig. 8. Cyclic voltammograms of ∼10^{-3} M solution of $[Co^{III}(L)_2]ClO_4$ (**1**) in acetonitrile: (a) at a scan rate 50 mV s^{-1} and (b) at different scan rates (only for the oxidation processes).

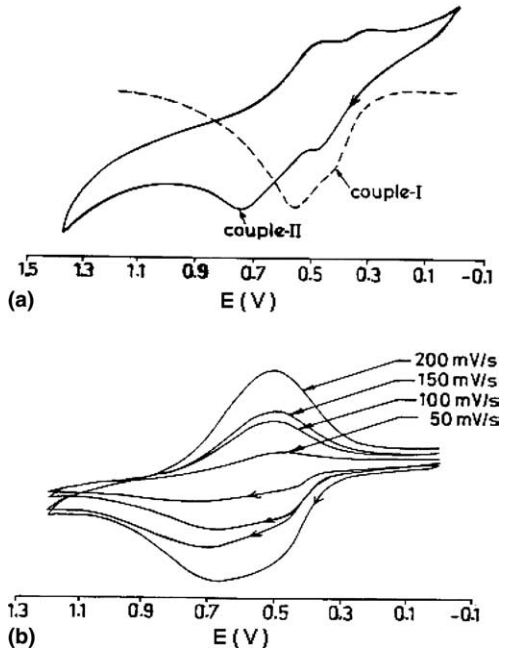

Fig. 9. Cyclic voltammograms of $\sim 10^{-3}$ M solution of $[Cu^{II}(L)\{OC(=O)CH_3\}]$ (**2**) in acetonitrile: (a) at a scan rate 20 mV s^{-1} and (b) at different scan rates (only for the oxidation processes).

precluded the isolation of the corresponding cobalt(II) analogue.

The complex **1** also displays two successive quasi-reversible oxidative responses, E^0, $V(\Delta E_p, \text{mV})$ at 0.64(80) (couple-I) and 0.83(120) (couple-II) (Fig. 8(a)). The one-electron nature of couple-I is confirmed by comparing its differential pulse voltammetric (dpv) current height with that of the Co(III)–Co(II) couple (couple-III). However, relative to couple-I or couple-III, the dpv current height of couple-II appears to be approximately three times greater.

On scan increment (>50 mV s^{-1}), the peaks of the two waves (couples I and II) broaden and merge to a single broad and blunt wave (Fig. 8(b)). The broadness of the profile of voltammograms particularly at a higher scan rate (>50 mV s^{-1}) reveals that the surface based adsorption processes are involved after the usual diffusion controlled based process [23]. In view of this serious electro deposition factor, repeated cleaning of electrode prior to each fresh run is found to be necessary.

The copper(II)-complex **2** shows two successive irreversible oxidation processes E_{pa} at 0.49 and 0.76 V versus SCE at a slower scan rate (20 mV s^{-1}) (Fig. 9(a)). However, on scan increment the shape of the voltammogram changes and at a higher scan rate (>100 mV s^{-1}) it appears to be an overlapping broad wave as like cobalt complex (Fig. 9(b)). Therefore, similar surface confinement processes are also involved during the oxidation steps particularly at a higher scan rate (>20 mV s^{-1}).

The electrogenerated oxidized species decomposes rapidly at room temperature, therefore, further characterization of the oxidized product and subsequent precise assignments of the oxidation processes have not been possible to make.

Since the free ligand (LH) exhibits one irreversible oxidation process at 0.56 V versus SCE in CH_3CN and +4 oxidation state of cobalt ion and +3 state of the copper ion are known to be difficult to stabilize, therefore, it may be logical to assign the oxidative responses as ligand-center based processes.

4. Conclusion

The use of sp^2-amido nitrogen containing tridentate ligand (L^-) leads to the formation of bis chelated octahedral complexes $[Co^{III}(L)_2]^+$ (**1**) and $[Zn^{II}(L)_2]$ (**3**). However, copper ion selectively stabilizes in square planar geometry having $Cu^{II}N_3O$ (**2**) chromophore. The basicity of the anionic sp^2-nitrogen center of L^- is such that it stabilizes the cobalt ion preferentially in trivalent Co^{III} state in **1** under atmospheric conditions. The strongly basic nature of L^- in **1** is also reflected in observed highly negative and reversible $Co^{III} \rightleftharpoons Co^{II}$ couple (−10 V versus SCE). The complexes exhibit strong charge-transfer transitions in UV–Vis region. Although no spin-allowed d–d transition has been observed for both cobalt and copper complexes, the cobalt complex **1** displays one very weak spin-forbidden $^1A_{1g} \rightarrow {}^3T_{1g}$ transition ($\varepsilon/M^{-1}\,cm^{-1}$, 11]) at 955 nm which has so far been rarely observed in few other octahedral Co(III) systems.

5. Supplementary material

Crystallographic data for the structural analysis have been deposited with the CCDC Nos. 216980, 216979 and 216978 for compounds LH, **1** and **2**, respectively. Supplementary data are available from the CCDC, 12 Union Road, Cambridge CB2 1EZ, UK

Acknowledgements

Financial support received from Council of Scientific and Industrial Research, New Delhi, India, is gratefully acknowledged. The X-ray structural studies were carried out at the National Single Crystal Diffractometer Facility, Indian Institute of Technology, Bombay. Special acknowledgement is made to Sophisticated Analytical Instrument Facility, Indian Institute of

Technology, Bombay for providing the NMR and EPR facilities.

References

[1] K.A. Jensen, P.H. Nielsen, Acta Chem. Scand. 18 (1964) 1.
[2] J.P. Puzas, R. Nakon, J.L. Petersen, Inorg. Chem. 25 (1986) 3837.
[3] J.C. Peters, S.B. Harkins, D.S. Brown, M.W. Day, Inorg. Chem. 40 (2001) 5083.
[4] S.B. Harkins, J.C. Peters, Organometallics 21 (2002) 1753.
[5] D.T. Sawyer, A. Sobkowiak, J.L. Roberts Jr., Electrochemistry for Chemists, Wiley, New York, 1995.
[6] G.M. Sheldrick, SHELXS 97, Program for Crystal Structure Solution and Refinement, University of Göttingen, Germany, 1997.
[7] (a) M. Tsukayama, C.R. Randall, F.S. Santillo, J.C. Dabrowiak, J. Am. Chem. Soc. 103 (1981) 458;
(b) S.J. Brown, M.M. Olmstead, P.K. Mascharak, Inorg. Chem. 28 (1989) 3720;
(c) J.D. Tan, E.T. Farinas, S.S. David, P.K. Mascharak, Inorg. Chem. 33 (1994) 4295;
(d) S.J. Brown, M.M. Olmstead, P.K. Mascharak, Inorg. Chem. 29 (1990) 3229;
(e) R.J. Guajardo, P.K. Mascharak, Inorg. Chem. 34 (1995) 802;
(f) R.J. Guajardo, J.D. Tan, P.K. Mascharak, Inorg. Chem. 33 (1994) 2838;
(g) S.J. Brown, S.E. Hudson, D.W. Stephan, P.K. Mascharak, Inorg. Chem. 28 (1989) 468;
(h) J.C. Dabrowiak, M.J. Tsukayama, J. Am. Chem. Soc. 103 (1981) 7543;
(i) Y. Sugiura, J. Am. Chem. Soc. 102 (1980) 5216;
(j) S.M. Hecht (Ed.), Bleomycin: Chemical, Biochemical and Biological Aspects, Springer-Verlag, New York, 1979.
[8] (a) B.K. Santra, G.K. Lahiri, J. Chem. Soc., Dalton Trans. (1997) 1883;
(b) A. Bharath, B.K. Santra, P. Munshi, G.K. Lahiri, J. Chem. Soc., Dalton Trans. (1998) 2643.
[9] (a) F.A. Chavez, J.M. Rowland, M.M. Olmstead, P.K. Mascharak, J. Am. Chem. Soc. 120 (1998) 9015;
(b) L.A. Tyler, J.C. Noveron, M.M. Olmstead, P.K. Mascharak, Inorg. Chem. 39 (2000) 357.
[10] C. Bombieri, E. Forsellini, A. Delpra, M.L. Tobe, C. Chatterjee, C.J. Cooksey, Inorg. Chim. Acta 75 (1983) 93.
[11] (a) F.A. Chavez, M.M. Olmstesd, P.K. Mascharak, Inorg. Chem. 36 (1997) 6323;
(b) T.J. Collins, R.D. Powell, C. Slebodnick, E.S. Uffelman, J. Am. Chem. Soc. 113 (1991) 8149;
(c) M. Ray, D. Ghosh, Z. Shirin, R.N. Mukherjee, Inorg. Chem. 36 (1997) 3568.
[12] (a) G.J. Palenik, Acta Crystallogr. 17 (1964) 687;
(b) R.G. Little, J.A. Moreland, D.B.W. Yawney, R.J. Doedens, J. Am. Chem. Soc. 96 (1974) 3834;
(c) R.G. Little, D.B.W. Yawney, R.J. Doedens, J. Chem. Soc., Chem. Commun. 4 (1972) 228;
(d) J.A. Bevan, D.P. Graddon, J.F. McConnell, Nature 199 (1963) 373.
[13] (a) T. Nakamura, H. Higuchi, K. Izutsu, Bull. Chem. Soc. Jpn. 62 (1989) 3089;
(b) R.L. Paul, S.M. Couchman, J.C. Jeffery, J.A. McCleverty, Z.R. Reeves, M.D. Ward, J. Chem. Soc., Dalton Trans. 6 (2000) 845.
[14] (a) B.K. Santra, G.K. Lahiri, J. Chem. Soc., Dalton Trans. (1997) 129;
(b) N. Bag, A. Pramanik, G.K. Lahiri, A. Chakravorty, Inorg. Chem. 31 (1992) 40.
[15] (a) I.K. Adzamili, K. Libson, J.D. Lydon, R.C. Elder, E. Deutsch, Inorg. Chem. 18 (1979) 303;
(b) B.A. Lange, K. Libson, E. Deutsch, R.C. Elder, Inorg. Chem. 15 (1976) 2985.
[16] (a) S. Chakraborty, M.G. Walawalkar, G.K. Lahiri, J. Chem. Soc., Dalton Trans. (2000) 2875;
(b) B. Mondal, H. Paul, V.G. Puranik, G.K. Lahiri, J. Chem. Soc., Dalton Trans. (2001) 481.
[17] A.B.P. Lever, Inorganic Electronic Spectroscopy, 2nd ed., Elsevier, Amsterdam, 1984, p. 463.
[18] (a) J.C. Jeffery, E. Schatz, M.D. Ward, J. Chem. Soc., Dalton Trans. (1992) 1921;
(b) N. Maki, Bull. Chem. Soc. Jpn. 42 (1969) 2275.
[19] K.C. Kalia, A. Chakravorty, Inorg. Chem. 7 (1968) 2016.
[20] (a) D.A. Johnson, A.G. Sharpe, J. Chem. Soc. A (1966) 798;
(b) C.K. Jorgensen, Adv. Chem. Phys. 5 (1963) 33.
[21] C. Jubert, A. Mohamadou, J. Marrot, J.P. Barbier, J. Chem. Soc., Dalton Trans. (2001) 1230.
[22] K. Delany, S.K. Arora, P.K. Mascharak, Inorg. Chem. 27 (1988) 705.
[23] R.S. Nicholson, I. Sharin, Anal. Chem. 36 (1964) 706.